

Undetected Past Contacts with Technological Species: Implications for Technosignature Science

CLAUDIO GRIMALDI^{1,2}

¹Laboratory of Statistical Biophysics, Ecole Polytechnique Fédérale de Lausanne – EPFL, 1015 Lausanne, Switzerland

²Centro Studi e Ricerche Enrico Fermi – CREF, Piazza del Viminale, 1, 00184 Roma, Italy

ABSTRACT

In the search for extraterrestrial intelligence (SETI), the highly incomplete sampling of the technosignature search space is often considered as a plausible explanation for the persistent lack of detections over six decades of searches. If correct, this would imply that technosignatures may already have reached Earth without being detected or correctly identified. Here, we explore this possibility using a Bayesian inference framework to estimate present-day detectability given $n \geq 1$ undetected contacts over the past 65 years – the period since the first SETI experiment. We show that achieving high detectability of technosignatures emitted within a few hundred light-years of Earth would require implausibly large n values, even exceeding the population of habitable planets within that range. More conservative estimates can be obtained only assuming that emitters are tightly clustered near Earth or that their population in the Milky Way has undergone a very recent and sudden boost. This tension is further exacerbated for short-lived technosignatures and persists whether they are omnidirectional, as in Dysonian megastructures, or directional, as in intentional communication attempts. These findings suggest that, if undetected past contacts from the Milky Way have indeed occurred, the best prospects of detection may lie in searches extending over several thousand light-years, though only a few detectable technoemissions would be expected.

1. INTRODUCTION

The search for technosignatures – remotely detectable indicators of extraterrestrial technology – has been ongoing for over sixty years, beginning with the first SETI experiment in 1960 (F. D. Drake 1961). Since then, more than 200 searches have been conducted³, targeting predominantly artificial radio signals, as well as optical and infrared emissions from beyond the Solar System, albeit less frequently and for only about fifty years. To date, however, no confirmed detections have been reported.

This lack of detection does not necessarily imply that humanity is the only technological civilization in the Galaxy. Rather, it may reflect that only a minute fraction of the vast multidimensional parameter search space has been explored so far (J. C. Tarter et al. 2010; J. T. Wright et al. 2018) – a situation compared to searching for a needle in a cosmic haystack (J. T. Wright et al. 2018). Consequently, the question of the prevalence, or even the existence, of advanced technological species in our Galaxy remains unresolved.

Even so, the absence of detections constitutes a valuable data point. While it does not constrain the existence of extraterrestrial technologies *per se*, it does inform us about upper limits on the prevalence of their detectable manifestations (J. E. Enriquez et al. 2017;

D. C. Price et al. 2020; B. S. Wlodarczyk-Sroka et al. 2020; V. Gajjar et al. 2022; G. W. Marcy et al. 2022; M. Suazo et al. 2022; J.-L. Margot et al. 2023; M. A. Garrett & A. P. V. Siemion 2022; Y. Uno et al. 2023; C. D. Tremblay & S. J. Tingay 2024; L. Manunza et al. 2025; L. A. Mason et al. 2024). In fact, to be potentially detectable, any technosignature must be observable from our vantage point at the time of observation. In particular, electromagnetic technosignatures (hereafter, technoemissions) emitted at some point in the past from elsewhere in the Galaxy must intersect Earth – an event referred to as “contact” in what follows – during the observational time window. Such a contact represents a necessary condition for potential detection (C. Grimaldi 2017; A. Balbi 2018). However, it is not a sufficient one, as factors such as signal strength, frequency characteristics, and distinguishability from background noise may still prevent actual detection.

From this perspective, possible explanations for the decades-long absence of detections can be classified into two broad categories: either technoemissions are sufficiently rare that none has illuminated Earth during the relatively brief 65 years of SETI searches, or they have indeed intersected our planet but have so far eluded detection – either because, for instance, they occurred at unmonitored wavelengths, were below instrumental sensitivity thresholds, or were recorded but not recognized as artificial.

The first scenario posits that Earth has not been traversed by extraterrestrial technoemissions over six

Email: claudio.grimaldi@epfl.ch

³ <https://technosearch.seti.org/>

decades, thereby rendering their detection impossible. Under fairly general assumptions, this premise would imply fewer than one to five such emissions per century generated across the entire Galaxy (C. Grimaldi 2023), suggesting that Earth is likely to remain unilluminated for at least several more decades.

The second possibility depicts a more optimistic scenario. If undetected or unrecognized contacts with technoemissions have occurred in the recent past, it is reasonable to expect that others may still be ongoing. This would imply that the necessary condition for detection is more likely to be met, thereby increasing the chances of discovery as future searches become more comprehensive and effective. Should the current, unprecedented commitment to the search for life elsewhere in general – and for technosignatures in particular – persists, this scenario suggests that a long-awaited discovery could be closer than ever.

Here, we quantitatively explore the implications of assuming that technoemissions generated across the Galaxy have intersected Earth since the first SETI experiment 65 years ago (F. D. Drake 1961). Using a Bayesian framework, we show that even a few technoemissions detectable today within relatively short distances from Earth ($\lesssim 1,000$ ly) would imply unrealistically large numbers of undetected past contacts. Extending the analysis to the entire Milky Way reduces the number of past contacts required to sustain significant present-day detectability. However, even in this case, detectable technoemissions are expected to be rare – only a few across the entire Galaxy – casting doubt on the prospect of a near-term detection.

By considering the possibility of past undetected contacts, this paper complements an earlier study (C. Grimaldi 2023), in which the absence of confirmed detections to date was attributed to a complete lack of contacts with technoemissions throughout the history of SETI.

2. MODEL OF TECHNOEMISSIONS

The model builds upon previous formulations (C. Grimaldi 2017; C. Grimaldi & G. W. Marcy 2018; C. Grimaldi 2023), which are briefly summarized below. We consider technoemissions to be generated within the Milky Way by technological species or their artifacts, hereafter collectively referred to as “emitters”. The spatial positions of these emitters are specified by the random variable \mathbf{r} , denoting their vector position relative to the Galactic center. It is further assumed that emitters are statistically independent, with an appearance rate per unit volume, $\gamma(\mathbf{r}, t)$, defined such that $\gamma(\mathbf{r}, t)d\mathbf{r}dt$ corresponds to the expected number of emitters within the elemental volume $d\mathbf{r}$ centered at \mathbf{r} that began emitting within a time interval dt centered at time t in the past (with $t > 0$ measuring backward times). According to this definition, the quantity $\Gamma(t) = \int d\mathbf{r} \gamma(\mathbf{r}, t)$ cor-

responds to the total appearance rate across the entire Galaxy at time t .

To model the scenario in which contacts with technoemissions have occurred over the past $\tau = 65$ yr, we start by considering an isotropic emitter that, at time t , generated a technoemission lasting for a duration L , propagating uniformly in all directions at the speed of light c . At the present time, the region covered by the radiation forms a spherical shell centered at \mathbf{r} , with outer and inner radii given by ct and $\max(ct - cL, 0)$,⁴ respectively (Fig. 1a). As illustrated in Fig. 1b, τ years ago this same spherical shell had outer and inner radii smaller by $c\tau$. If, during this interval, the distance to the emitter lay between the inner radius from τ years ago, $\max(ct - cL - c\tau, 0)$, and the current outer radius ct , then the technoemission would have intersected Earth at some point within the past τ years (Fig. 1c). This translates into the following condition on the appearance time:

$$d/c \leq t \leq d/c + L + \tau, \quad (1)$$

where $d = |\mathbf{r} - \mathbf{r}_o|$ denotes the distance between the emitter and Earth, located at \mathbf{r}_o .

Integrating $\gamma(\mathbf{r}, t)$ over t and \mathbf{r} under the constraint imposed by Equation (1) yields the mean number of contacts with technoemissions of duration L that have occurred within the past τ years. Assuming that the technoemission lifetimes follow a probability distribution function (PDF) $\rho_L(L)$, and focusing on emitters located within a distance R from Earth, the corresponding expected number $\eta(\tau, R)$ of technoemissions intersecting Earth is given by:

$$\eta(\tau, R) = \int dL \rho_L(L) \int d\mathbf{r} \int_{d/c}^{d/c+L+\tau} dt \gamma(\mathbf{r}, t) \theta(R - d) \quad (2)$$

where $\theta(x)$ is the Heavyside step function.

The isotropic technoemission model described above applies to Dysonian megastructures (F. J. Dyson 1960), which are expected to radiate in the infrared, and to other omnidirectional radio or optical signals. Spectral technosignatures from the atmospheres of exoplanets can be considered another example of omnidirectional technoemissions (H. W. Lin et al. 2014; R. Kopparapu et al. 2021; J. Haqq-Misra et al. 2022a), as their transmitted or reflected starlight is not directed toward specific targets. However, we do not count them among the potentially missed signals throughout SETI history, since searches for them have just become barely possible (S. Seager et al. 2025). Likewise, we do not consider technoemissions produced by modifications of exoplanetary surfaces through intensive artificial illumination (T. G. Beatty 2022) or selectively engineered absorption/reflection of starlight (M. Lingam & A. Loeb 2017a;

⁴ For $t < L$, the inner radius is zero, meaning that the radiation fills a spherical region of radius ct

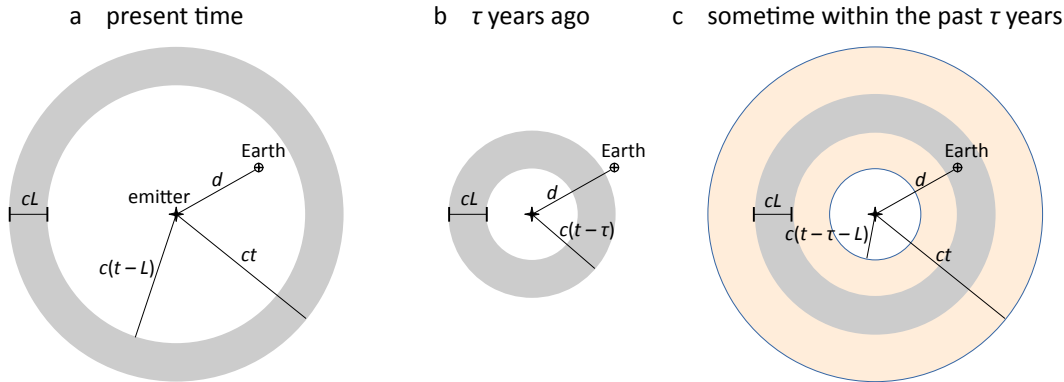


Figure 1. Temporal evolution of a spherical shell produced by an isotropic technoemission of duration L . In the present-day configuration (panel a), the outer and inner radii of the shell are ct and $c(t - L)$, respectively; the example shown corresponds to the case in which Earth lies inside the hollow region of the shell, at a distance d from the emitter. In panel b, the same shell is shown τ years ago, when the outer and inner radii were smaller by $c\tau$ and Earth was outside the shell. In panel c, the shell has intersected Earth at some point over the past τ years if $c(t - \tau - L) \leq d \leq ct$. Expressed in terms of the emitter appearance time t , this condition becomes $d/c \leq t \leq d/c + L + \tau$, yielding an appearance time window for intersection of $L + \tau$.

S. V. Berdyugina & J. R. Kuhn 2019; B. Jaiswal 2023), as no dedicated searches have yet been conducted (J. Haqq-Misra et al. 2022b).

The present omnidirectional model for technoemissions can be generalized to include directional signals, such as those produced by unidirectional beacons targeting other planetary systems, interstellar propulsion (J. N. Benford & D. J. Benford 2016; M. Lingam & A. Loeb 2017b), or communication between spacecrafts (R. N. Bracewell 1960). In this case, contact would occur only with those beacons whose beamwidth intersects Earth. Here, we make the simplifying assumption that the orientation and beamwidth of such directional signals are independent of the emitters' time of appearance, position, and longevity. Under this assumption, their contribution can be encoded by an anisotropic prefactor $\chi \leq 1$ applied to the right-hand side of Equation (2), reflecting the lower probability for a directional technoemission to intersect Earth's line of sight compared to an isotropic one with the same occurrence rate and longevity (C. Grimaldi 2017, 2023).

In writing the probability distribution of contacts, we do not impose a strict upper limit on the population of emitters in the Galaxy, requiring only that the number of contacts remains much smaller than the estimated $\sim 10^{10}$ potentially habitable planets in the Milky Way (S. Bryson et al. 2020)⁵. In this way, owing to the statistical independence of the emitters, the probability that exactly n technoemissions have intersected Earth over the past τ years from within a distance R follows a Poisson distribution (C. Grimaldi 2023; C. Grimaldi & G. W.

Marcy 2018):

$$P(n; \tau, R) = \frac{[\eta(\tau, R)]^n}{n!} e^{-\eta(\tau, R)}. \quad (3)$$

2.1. Stationary regime

Proceeding further requires modeling the rate per unit volume, $\gamma(\mathbf{r}, t)$, for which we lack prior knowledge, except from the requirements that emitter positions must lie within the Milky Way and that their appearance times cannot precede the birth of the Galaxy itself (~ 13.8 Gyr ago). Here, we focus primarily on the instructive case of a stationary regime, in which $\gamma(\mathbf{r}, t)$ is independent of the appearance time t . This assumption is justified by noting that, in Equation (1), the interval during which technoemissions intersect Earth is $L + \tau$: if $\rho_L(L)$ is such that, within this interval, the time dependence of $\gamma(\mathbf{r}, t)$ is sufficiently weak or negligible, then $\gamma(\mathbf{r}, t)$ can be approximated as $\Gamma \rho_E(\mathbf{r})$, where Γ is the appearance rate of emissions across the entire Galaxy and $\rho_E(\mathbf{r})$ denotes the PDF of the emitter positions, normalized to unity. Within this stationary regime, the integration over t in Equation (2) yields $\eta(\tau, R) = \pi_R \chi \Gamma (\bar{L} + \tau)$, so Equation (3) reduces to:

$$P(n; \Gamma, \tau, \pi_R) = \frac{[\pi_R \chi \Gamma (\bar{L} + \tau)]^n}{n!} e^{-\pi_R \chi \Gamma (\bar{L} + \tau)} \quad (4)$$

where $\bar{L} = \int dL \rho_L(L) L$ is the average longevity of the technoemissions and

$$\pi_R = \int d\mathbf{r} \rho_E(\mathbf{r}) \theta(R - |\mathbf{r} - \mathbf{r}_o|) \quad (5)$$

represents the probability of an emitter being within a distance R from Earth (C. Grimaldi 2017). Regardless of the specific distribution of emitters, π_R increases

⁵ By ‘‘habitable planets’’ we mean rocky worlds orbiting within the habitable zones of FGK stars

monotonically with R , from $\pi_R = 0$ at $R = 0$ and reaching unity as R becomes larger than the characteristic size of the Milky Way.

2.2. Bayesian analysis

Our objective is to infer the emission rate, Γ , from the hypothetical scenario, denoted $\mathcal{U}_{n,\tau}$, in which n undetected contacts have occurred over the past τ years. To this end, we adopt a Bayesian inference approach, using Equation (4) as the basis for constructing the likelihood function of $\mathcal{U}_{n,\tau}$ given Γ . In so doing, we note that the working hypothesis – namely, that these n contacts have gone undetected – implies that the associated technoemissions were such as to elude our search efforts. This could be due to various factors, such as their wavelength, position in the sky, or other characteristics, but in particular because their signals may have been too faint or emitted from distances beyond the sensitivity limits of our telescopes. In such a scenario, the undetected technoemissions could have originated anywhere within the Galaxy. The corresponding likelihood function, $P(\mathcal{U}_{n,\tau}|\Gamma)$, is therefore provided by Equation (4) with $\pi_R = 1$:

$$P(\mathcal{U}_{n,\tau}|\Gamma) = P(n; \Gamma, \tau, 1). \quad (6)$$

Bayes’ theorem allows us to derive the posterior PDF of Γ under the assumption that the scenario $\mathcal{U}_{n,\tau}$ has occurred:

$$p(\Gamma|\mathcal{U}_{n,\tau}) = \frac{P(\mathcal{U}_{n,\tau}|\Gamma)p(\Gamma)}{\int d\Gamma P(\mathcal{U}_{n,\tau}|\Gamma)p(\Gamma)}, \quad (7)$$

where $p(\Gamma)$ is the prior PDF encoding our assumptions about the possible values of Γ before taking the n contacts into account. In what follows, we assume complete prior ignorance and adopt a log-uniform prior, $p(\Gamma) \propto 1/\Gamma$, which assigns equal weight to all orders of magnitude of Γ . Under this assumption, the posterior PDF takes the form of a Gamma distribution for Γ :

$$p(\Gamma|\mathcal{U}_{n,\tau}) = \chi(\bar{L} + \tau) \frac{[\chi\Gamma(\bar{L} + \tau)]^{n-1}}{(n-1)!} e^{-\chi\Gamma(\bar{L} + \tau)}. \quad (8)$$

The corresponding posterior expectation value of the technoemission rate is then (Appendix A):

$$\langle \Gamma \rangle = \chi^{-1} \frac{n}{\bar{L} + \tau}, \quad (9)$$

which increases with the number n of past contacts and decreases as the average longevity \bar{L} of technosignatures increases. This behavior has a clear physical interpretation, stemming directly from the contact condition in Equation (1): the appearance time interval during which a technoemission of average duration \bar{L} can intersect Earth is $\bar{L} + \tau$. Consequently, n contacts within the same interval must occur at a rate scaling as $n/(\bar{L} + \tau)$. The prefactor $\chi^{-1} \geq 1$ in Equation (9) compensates for the reduced intersection probability of anisotropic technoemissions.

3. RESULTS AND DISCUSSION

3.1. Present-day detectability of technoemissions

Having established the impact of past undetected contacts on the rate of technoemissions, we next explore how such past contacts influence technoemission detectability today. By “detectability”, we mean the capability of present-day and near-future telescope technologies to detect a technoemission. This capability has considerably advanced in recent years, particularly in terms of the range of searched wavelengths, sensitivity thresholds, and survey speeds (C. D. Tremblay & S. J. Tingay 2024; L. Manunza et al. 2025; L. A. Mason et al. 2024; J. Maire et al. 2022; X.-H. Luan et al. 2023; C. D. Tremblay et al. 2025). To appreciate the importance of recent efforts, it suffices to note that since its launch in 2016, Breakthrough Listen has explored a parameter space largely exceeding that of all previous searches combined over the preceding fifty years (M. A. Garrett & A. P. V. Siemion 2022). Looking ahead, upcoming facilities – such as the Square Kilometre Array (SKA) and the Next Generation Very Large Array (ngVLA) – promise to significantly enhance the observational prospects for technosignature science (A. Siemion et al. 2015; C. Ng et al. 2022).

In the following, we define a technoemission intersecting Earth as detectable if its emitter lies within a distance R from our planet. This criterion conveniently encapsulates both the intrinsic properties of the emission and the instrumental detection capabilities within a single parameter. A radio or microwave signal with an effective isotropic radiated power W is potentially detectable up to a distance $R = \sqrt{W/4\pi S_{\min}}$, where S_{\min} denotes the minimum detectable flux, determined by factors such as bandwidth, integration time, and other instrumental parameters (J. E. Enriquez et al. 2017). For optical or infrared technoemissions, the maximum detectable distance R is likewise determined by the intrinsic properties of the emission as well as by instrumental specifications (A. W. Howard et al. 2004).

To account for the diversity of such specifications and emission characteristics, R is treated here as a free parameter. Accordingly, Equation (4) with $\pi_R \leq 1$ and $\tau = 0$ yields the probability that exactly $k = 0, 1, 2, \dots$ technoemissions, generated at a constant rate Γ , are detectable at the present time (event \mathcal{D}_k) (C. Grimaldi & G. W. Marcy 2018):

$$P(\mathcal{D}_k|\Gamma) = P(k; \Gamma, 0, \pi_R). \quad (10)$$

Marginalizing $P(\mathcal{D}_k|\Gamma)$ with respect to the posterior PDF of Γ yields the posterior distribution of k detectable contacts, conditional on the occurrence of $n \geq 1$

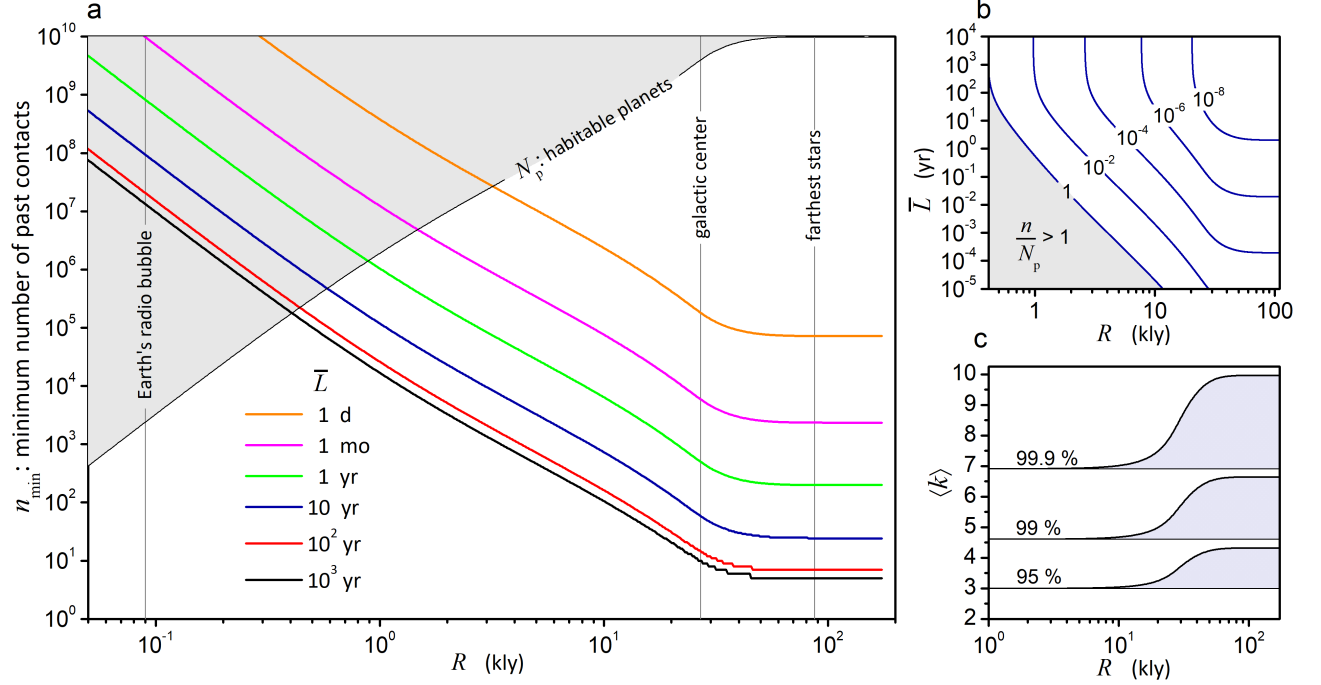


Figure 2. Results assuming undetected contacts with technoemissions over the past 65 years. a: Number n of undetected past contacts required to achieve a present-day detectability of at least 95 %, as a function of the search radius R . The thin black line shows the number of habitable planets N_p as a function of R calculated from $N_p = 10^{10} \int d\mathbf{r} \rho_{\text{disk}}(\mathbf{r}) \theta(R - d)$, where d is the distance from Earth. The grey region marks where $n > N_p$. b: Average emitter longevity versus R for selected n/N_p values. c: Upper and lower bounds on the expected number of present-day detections, $\langle k \rangle$, computed from Equation (15) for detectabilities $\mathcal{P} = 95\%$, 99% , and 99.9% . For each \mathcal{P} , all possible $\langle k \rangle$ values lie within the corresponding colored areas.

undetected contacts over the past τ years:

$$P(\mathcal{D}_k | \mathcal{U}_{n,\tau}) = \int_0^\infty d\Gamma P(\mathcal{D}_k | \Gamma) p(\Gamma | \mathcal{U}_{n,\tau}) \\ = \frac{(\pi_R \bar{L})^k (\bar{L} + \tau)^n (n + k - 1)!}{[\bar{L}(1 + \pi_R) + \tau]^{k+n} k!(n-1)!}. \quad (11)$$

Notably, $P(\mathcal{D}_k | \mathcal{U}_{n,\tau})$ is independent of the anisotropy factor χ (Appendix B). This arises because the detection probability of a directional signal is reduced by a factor χ , exactly compensating for the χ^{-1} enhancement of its occurrence rate. Consequently, all results derived from (11) apply equally to both isotropic and directional technoemissions, as well as to a mixture of them⁶.

We define the present-day detectability as the probability \mathcal{P} of at least one detectable contact occurring today:

$$\mathcal{P} = 1 - P(\mathcal{D}_{k=0} | \mathcal{U}_{n,\tau}) = 1 - \left(\frac{\bar{L} + \tau}{\bar{L}(1 + \pi_R) + \tau} \right)^n, \quad (12)$$

For any given value of the search radius R and the average longevity \bar{L} , \mathcal{P} is a strictly increasing function of n .

⁶ This may not hold true when considering mixtures of isotropic and anisotropic signals having differing longevitys.

While this aligns with our intuition – the more contacts there have been in the past, the greater the probability of detection today – it also raises a more intriguing and relevant question for technosignature science: How many contacts must have gone undetected over the past $\tau = 65$ years for there to be a high probability of detection today?

Figure 2 provides an initial answer by showing the minimum number n_{min} of past undetected contacts required to ensure at least a 95 % probability that technosignals are detectable within a distance R from Earth. n_{min} is readily obtained by inverting Equation (12):

$$n_{\text{min}} = \left\lceil \frac{\ln(1 - \mathcal{P})^{-1}}{\ln\left(\frac{\bar{L}(1 + \pi_R) + \tau}{\bar{L} + \tau}\right)} \right\rceil, \quad (13)$$

where $\lceil \dots \rceil$ denotes the ceiling function, showing that n_{min} reaches its minimum value when $\pi_R \rightarrow 1$, whereas it becomes unbounded in the limit $\pi_R \rightarrow 0$ (i.e., $R \rightarrow 0$). The calculations shown in Fig. 2 assume that the distribution of emitters, $\rho_E(\mathbf{r})$, follows that of stars in the galactic thin disk, denoted $\rho_{\text{disk}}(\mathbf{r})$, which is modeled by a double exponential with a radial scale length of 2.5 kpc (8.15 kly) and a vertical scale length of 0.16 kpc

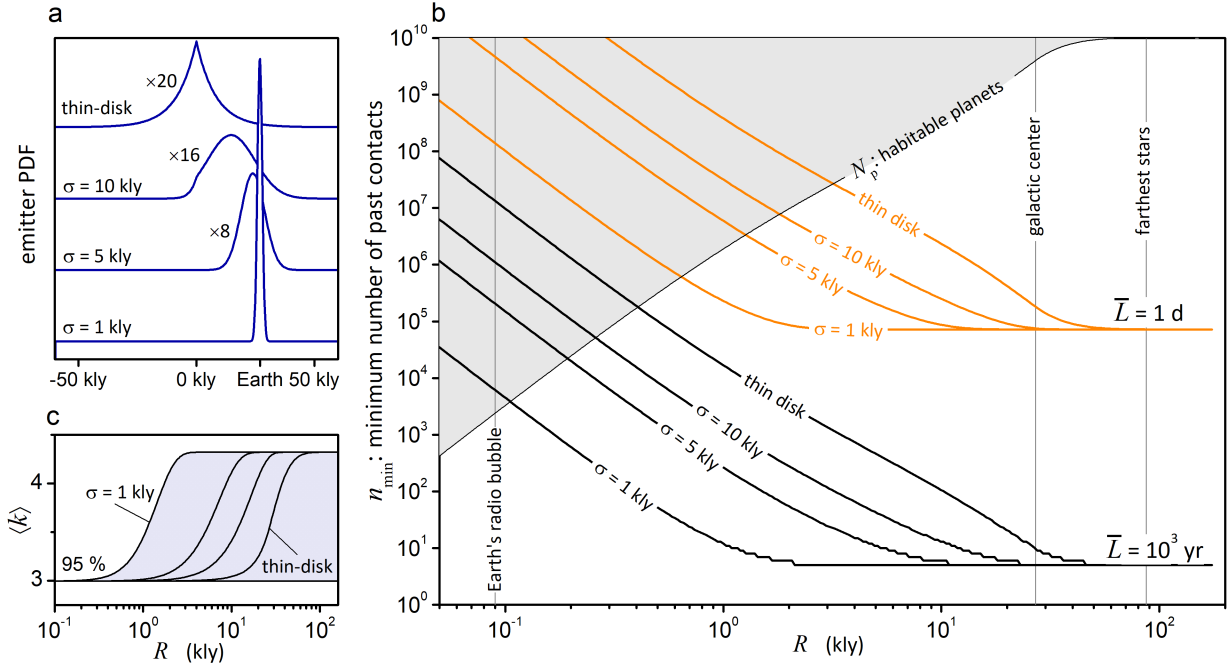


Figure 3. Effects of emitter clustering around Earth on past undetected contacts. a: Profile of the emitter PDF as a function of the radial distance from the galactic center for different values of the standard deviation σ . b: Number n of undetected past contacts required to achieve a present-day detectability \mathcal{P} of at least 95 %, as a function of the search radius R . c: Upper and lower bounds on $\langle k \rangle$ computed from Equation (15) for $\mathcal{P} = 95$ %

(0.52 kly) (T. C. Licquia & J. A. Newman 2016; P. J. McMillan 2016).

In Figure 2a, n_{\min} is lowest when the search radius covers the entire galactic disk ($R \gtrsim 60$ kly), ranging from $n_{\min} = 5$ for $\bar{L} \geq 10^3$ yr to as many as $n_{\min} \simeq 10^5$ for technoemissions lasting only one day on average – and even higher for shorter durations. These values remain far smaller than the estimated $\sim 10^{10}$ habitable planets around FGK stars, which we take as a proxy for the maximally conceivable – albeit highly implausible – number of potential emitters. However, as the search radius decreases, the number of undetected contacts rises steadily to maintain $\mathcal{P} \geq 95$ %, eventually surpassing even the number $N_p = 10^{10} \int d\mathbf{r} \rho_{\text{disk}}(\mathbf{r}) \theta(R - d)$ of habitable planets within the same range.

This provides a first important insight into our chances of detecting technosignatures. Even under the overly optimistic assumption of one emitter per 100 habitable planets, the results shown in Figs. 2a and 2b imply that detectable (i.e., $\mathcal{P} \geq 95$ %) long-lived emitters must lie at distances beyond $\sim 1,000$ ly from Earth, or beyond $\sim 10,000$ ly in the case of short-lived ones. These thresholds correspond to $\sim 10^4$ long-lived undetected contacts over the past 65 years (i.e., roughly one every two days) or $\sim 10^6$ short-lived ones (about 40 per day). More conservative – and arguably more plausible – rates of past contacts would push these minimal distances even farther. For example, less than one undetected contact per year ($n_{\min} \leq 65$) would be achieved

only for $R \gtrsim 12,000$ ly in the case of long-lived technoemissions.

A less stringent detectability requirement does not significantly alter these conclusions. For example, at fixed R , reducing the detectability threshold in Equation (13) from $\mathcal{P} \geq 95$ % to $\mathcal{P} \geq 50$ % decreases n_{\min} by only a factor of ~ 4 .

3.2. Average number of present-day detectable technoemissions

A second key result pertains the expected number of present-day detectable technoemissions, given $n \geq 1$ past contacts. This is obtained by summing $kP(\mathcal{D}_k | \mathcal{U}_{n,\tau})$ over all $k \geq 0$, yielding (Appendix C):

$$\langle k \rangle = \frac{\pi_R \bar{L}}{\bar{L} + \tau} n, \quad (14)$$

implying that $\langle k \rangle$ grows indefinitely with the number of past contacts. However, when combined with Equation (12), it can be shown that the expected number of detectable technoemissions is bounded as (Appendix C):

$$\ln(1 - \mathcal{P})^{-1} \leq \langle k \rangle \leq \frac{\pi_R \ln(1 - \mathcal{P})^{-1}}{\ln(1 + \pi_R)}, \quad (15)$$

showing that $\langle k \rangle$ actually increases only logarithmically with the detection probability \mathcal{P} . Even in the case of almost certain detectability (e.g., $\mathcal{P} = 99.9$ %), $\langle k \rangle$ remains below 10, regardless of the search radius (Fig.

2c). Thus, while increasing R helps reduce the number of undetected past contacts to more conservative values, it also greatly expands the search volume – potentially to galactic scales – within which, however, only a few detectable technoemissions might be expected among an astronomically large number of stars.

This trade-off points to an optimal search radius of at least a few thousand light-years, a range that is, in principle, accessible to the FAST telescope (X.-H. Luan et al. 2023) or the eventual completion of the SKA (A. Siemion et al. 2015) and the ngVLA (C. Ng et al. 2022), provided the technoemissions are sufficiently powerful (at least an EIRP equivalent to that of the Arecibo telescope) and long-lived.

3.3. Insensitivity to the prior

The requirement of past contacts, encoded in the likelihood function, makes the above results largely insensitive to the choice of the prior, even for informative ones. For instance, adopting a prior PDF for Γ of the form $p(\Gamma) \propto \Gamma^{\alpha-1}$ – ranging from optimistic ($\alpha \simeq 1$) to pessimistic ($\alpha \simeq -1$) beliefs about the possible values of Γ (D. S. Spiegel & E. L. Turner 2012; C. Grimaldi 2023) – would only replace n by $n + \alpha$ in the formulas for \mathcal{P} and $\langle k \rangle$, leaving the results in Fig. 2 essentially unchanged for n sufficiently large. Thus, the conclusions drawn above remain valid even under substantially different prior assumptions.

3.4. Effects of spatio-temporal dependences of emission rates

A potential limitation of the above analysis stems from the assumption of a stationary rate of technoemissions from emitters uniformly distributed across the thin disk of the Milky Way. Depending on the evolutionary history of technological species in our Galaxy, the spatio-temporal distribution of emitters may deviate significantly from this idealized scenario (M. M. Ćirković 2004; A. Balbi & M. M. Ćirković 2021), leading to a broad range of possible configurations that could affect the conclusions drawn in the previous section.

Here, we focus on cases that allow for high present-day detectability at distances shorter than several thousand light-years, without requiring an implausibly large number of past contacts. Our main objective is to assess to what extent these cases represent a viable alternative to the results shown in Fig. 2.

We begin by examining a significant deviation from a uniform emitter distribution across the thin disk, which could result from regions of the Galaxy more favorable to the development of advanced civilizations or from higher local prevalence of space probes. Specifically, we consider emitters to be more or less localized around Earth, following a PDF of the form $\rho_E(\mathbf{r}) \propto \rho_{\text{disk}}(\mathbf{r})e^{-d^2/2\sigma^2}$, where, as before, $\rho_{\text{disk}}(\mathbf{r})$ is the spatial PDF of stars in the thin disk. The rationale for this choice is that for a high local concentration of emitters (i.e., small σ),

the number of past contacts required to achieve a given detectability \mathcal{P} is expected to level off well before R reaches the scale of the Galactic disk, since the emitter distribution decreases rapidly beyond $R \sim \sigma$.

This trend is confirmed by the results shown in Fig. 3b: n_{min} decreases systematically as emitters become more localized around Earth. However, achieving both high detectability ($\mathcal{P} \geq 95\%$) and more plausible numbers of past contacts at relatively short distances requires emitters to be tightly clustered around Earth. For instance, fewer than one long-lived past contact per year ($n_{\text{min}} \lesssim 65$) is attainable for $R \gtrsim 500$ ly if almost all emitters are long-lived and located within 1,000 light years of Earth (Fig. 3a), corresponding to merely $\sim 0.02\%$ of the thin-disk volume. Even tighter emitters localizations would be required to attain similar frequencies of past contacts from short-lived emitters. Notably, the bounds on the present-day number of detectable technoemissions remain relatively unaffected by the localization parameter σ (Fig. 3c).

Another hypothetical scenario that could yield realistic values of n on length scales well below that of the Galaxy is one in which the emitter birthrate has increased in the relatively recent past (M. M. Ćirković 2004). Such an increase could result from large-scale colonization events (M. Lingam 2016; J. Carroll-Nellenback et al. 2019) or from the abandonment of a non-interference directive – such as the one envisioned by the zoo hypothesis (J. A. Ball 1973; I. A. Crawford & D. Schulze-Makuch 2024) – in which advanced alien civilizations deliberately avoid contact to preserve the natural development of less advanced societies. A secular increase of the emitter birthrate may also result from astrobiological phase transition scenarios (M. M. Ćirković & B. Vukotić 2008), in which the gradual decline of global catastrophic events such as gamma-ray bursts (J. Annis 1999) may have only recently allowed the emergence of technological species in the Milky Way.

Although the aforementioned scenarios describe some specific mechanisms for a temporal increase of the emitter birthrates, the possible causes and the details of such a transition are of secondary importance for our analysis. Here, we consider a simplified model in which the Galaxy is virtually devoid of emitters for $t > t_c$ and becomes populated for $t < t_c$, where t_c denotes the timescale of the transition. To this end, we adopt a separable form for the appearance rate per unit volume, $\gamma(\mathbf{r}, t) = \Gamma(t)\rho_{\text{disk}}(\mathbf{r})$, where $\Gamma(t) \propto 1/[e^{\beta(t-t_c)} + 1]$ is normalized such that $\Gamma(t=0) = \Gamma$. For illustration, we set the growth rate to $\beta = 1 \text{ kyr}^{-1}$ (Fig. 4a).

Figure 4b shows that the number of past contacts from emitters located beyond $\sim ct_c$ quickly reaches its lower bound as a function of R , in analogy with the spatial localization case considered above. However, achieving a significant reduction of n_{min} , while maintaining a high detectability today, requires a very recent increase in the

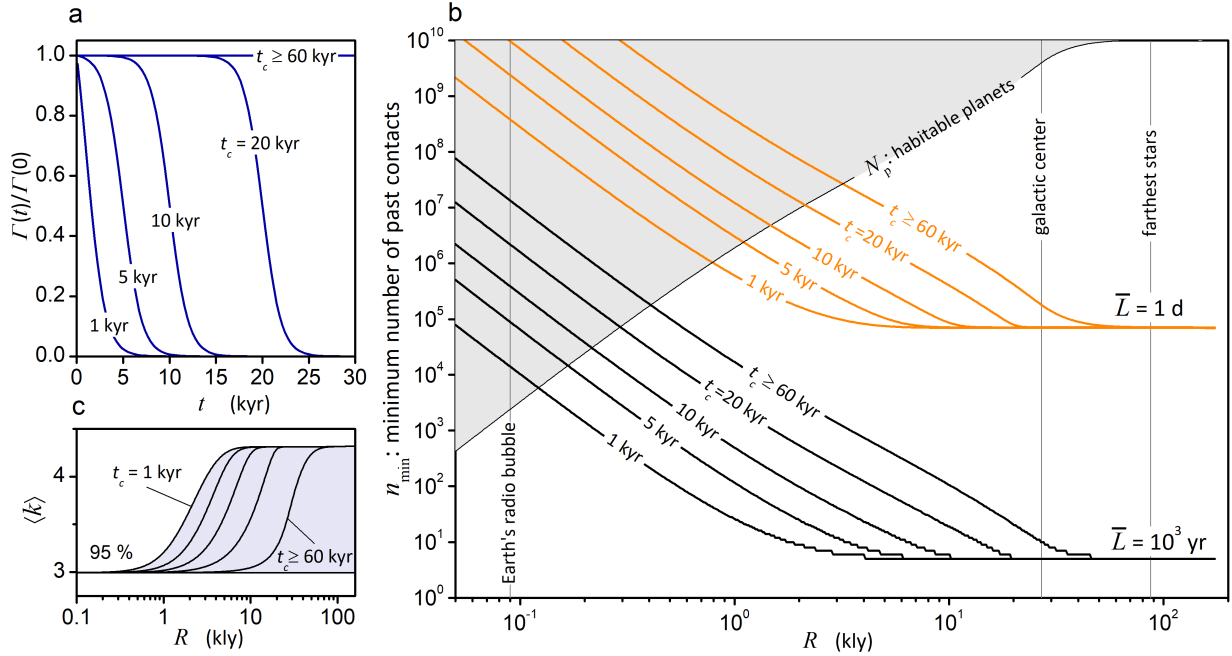


Figure 4. Effects of a temporal transition toward a high emitter birthrate on the number of undetected past contacts. a: Dependence of emitter appearance time for different transition times t_c . The growth rate is fixed at 1 kyr^{-1} . b: Corresponding minimum number n_{\min} of undetected past contacts required to achieve a present-day detectability \mathcal{P} of at least 95 %. c: Upper and lower bounds on $\langle k \rangle$ computed from Equation (15) for $\mathcal{P} = 95 \%$.

emitter population. For instance, to achieve $n_{\min} \lesssim 65$ for $R \gtrsim 600 \text{ ly}$ in the case of long-lived technoemissions, the transition must have occurred only $\sim 1 \text{ kyr}$ ago – that is, during historical times for humanity – with no significant change in $\langle k \rangle$ (Fig. 4c). Growth rates slower than $\beta \sim 0.1 \text{ kyr}^{-1}$, as would be expected for large-scale colonization or astrophysical phase transitions, would effectively recover the stationary scenario of Fig. 2.

The key result from Figs. 3 and 4 is that avoiding untenably large numbers of past contacts at small search radii requires invoking no less implausible scenarios, such as emitters confined to our immediate vicinity or a very recent and sudden increase in their population. These findings reinforce our conclusion that assuming undetected contacts throughout SETI’s history does not necessarily imply a high detection probability today ($\mathcal{P} \geq 95\%$), unless emitters are long-lived and located several thousand light-years from Earth. Even then, the expected number of detectable technoemissions increases only logarithmically with \mathcal{P} , suggesting that, even with near-certain detectability and precise knowledge of what to search for across the vast parameter search space, at most a few would be expected in the entire Milky Way.

Before concluding, a few remarks are in order regarding the general applicability of our model to scenarios other than the distributions of emitters in our Galaxy considered here. In principle, our formalism could be adapted to account for intergalactic technoemissions. In such a case, however, the emitter distribution $\rho_E(\mathbf{r})$ would need to be appropriately modeled, and the resulting estimates of the number of past undetected contacts would have to be compared to plausibility parameters different from the number N_p of habitable exoplanet in our Galaxy. Likewise, in considering the possibility of emitters in our immediate neighborhood – particularly technoemissions from artifacts in the Solar System or within a few light-years from Earth – N_p would cease to be a meaningful parameter for assessing the plausibility of such a scenario, and alternative benchmarks would need to be considered.

ACKNOWLEDGMENTS

CG is grateful to the referee for constructive suggestions that significantly improved the manuscript, and for helpful discussions with Amedeo Balbi, Paolo De Los Rios, and Huckleberry David Gaston Thums.

APPENDIX

A. CONDITIONAL EXPECTATION OF THE EMISSION RATE

The expected value of Γ , conditional on $n \geq 1$ past contacts, is obtained from the posterior PDF in (8):

$$\langle \Gamma \rangle = \int_0^\infty d\Gamma \Gamma p(\Gamma | \mathcal{U}_{n,\tau}) = \int_0^\infty d\Gamma \frac{[\chi \Gamma (\bar{L} + \tau)]^n}{(n-1)!} e^{-\chi \Gamma (\bar{L} + \tau)}. \quad (\text{A1})$$

After changing the integration variable to $x = \chi \Gamma (\bar{L} + \tau)$ and using $\int_0^\infty dx x^n e^{-x} = n!$, (A1) reduces to:

$$\langle \Gamma \rangle = \chi^{-1} \frac{n}{\bar{L} + \tau}. \quad (\text{A2})$$

B. INDEPENDENCE OF THE PRESENT-DAY DETECTABILITY ON TECHNOEMISSION ANISOTROPY

The probability of k detectable contacts, conditional on the occurrence of $n \geq 1$ undetected contacts over the past τ years, is given by the following predictive posterior distribution:

$$P(\mathcal{D}_k | \mathcal{U}_{n,\tau}) = \int_0^\infty d\Gamma P(\mathcal{D}_k | \Gamma) p(\Gamma | \mathcal{U}_{n,\tau}) = \frac{1}{k!(n-1)!} \int_0^\infty d\Gamma (\chi \pi_R \Gamma \bar{L})^k \chi (\bar{L} + \tau) [\chi \Gamma (\bar{L} + \tau)]^{n-1} e^{-\chi \Gamma [\bar{L}(1+\pi_R) + \tau]}. \quad (\text{B3})$$

Setting the integration variable to $x = \chi \Gamma$ makes the integral independent of the anisotropy factor χ . This stems from a perfect compensation: the χ^{-1} -amplification of the emission rate (A2) is canceled by the factor χ in the detection probability. A further change of the integration variable then yields:

$$P(\mathcal{D}_k | \mathcal{U}_{n,\tau}) = \frac{(\pi_R \bar{L})^k (\bar{L} + \tau)^n}{[\bar{L}(1 + \pi_R) + \tau]^{k+n}} \frac{\int_0^\infty dx x^{n+k-1} e^{-x}}{k!(n-1)!} = \frac{(\pi_R \bar{L})^k (\bar{L} + \tau)^n}{[\bar{L}(1 + \pi_R) + \tau]^{k+n}} \frac{(n+k-1)!}{k!(n-1)!}. \quad (\text{B4})$$

C. BOUNDS ON $\langle K \rangle$

The average number of present-day detectable technoemissions, conditioned to n past contacts, is obtained from:

$$\langle k \rangle = \sum_{k=0}^\infty k P(\mathcal{D}_k | \mathcal{U}_{n,\tau}) = \sum_{k=0}^\infty k \int_0^\infty d\Gamma P(\mathcal{D}_k | \Gamma) p(\Gamma | \mathcal{U}_{n,\tau}). \quad (\text{C5})$$

Moving the sum over k inside the integral and using (A1) and (A2) yields:

$$\langle k \rangle = \int_0^\infty d\Gamma \left[\sum_{k=0}^\infty k P(\mathcal{D}_k | \Gamma) \right] p(\Gamma | \mathcal{U}_{n,\tau}) = \chi \pi_R \bar{L} \langle \Gamma \rangle = \frac{\pi_R \bar{L}}{\bar{L} + \tau} n. \quad (\text{C6})$$

To find upper and lower bounds on $\langle k \rangle$, we use (12) to express n in terms of the detection probability \mathcal{P} and rewrite (C6) as:

$$\langle k \rangle = \frac{\pi_R \bar{L}}{\bar{L} + \tau} \frac{\ln(1 - \mathcal{P})^{-1}}{\ln\left(1 + \frac{\pi_R \bar{L}}{\bar{L} + \tau}\right)}. \quad (\text{C7})$$

For fixed \mathcal{P} , $\langle k \rangle$ is a continuous increasing function of \bar{L} , with lower and upper limits given respectively by:

$$\lim_{\bar{L}=0} \langle k \rangle = \ln(1 - \mathcal{P})^{-1}, \quad \text{and} \quad \lim_{\bar{L}=\infty} \langle k \rangle = \frac{\pi_R \ln(1 - \mathcal{P})^{-1}}{\ln(1 + \pi_R)}. \quad (\text{C8})$$

REFERENCES

- Annis, J. 1999, *Journal of the British Interplanetary Society*, 52, 19, doi: [10.48550/arXiv.astro-ph/9901322](https://doi.org/10.48550/arXiv.astro-ph/9901322)
- Balbi, A. 2018, *Astrobiology*, 18, 54, doi: [10.1089/ast.2017.1652](https://doi.org/10.1089/ast.2017.1652)
- Balbi, A., & Ćirković, M. M. 2021, *The Astronomical Journal*, 161, 222, doi: [10.3847/1538-3881/abec48](https://doi.org/10.3847/1538-3881/abec48)
- Ball, J. A. 1973, *Icarus*, 19, 347, doi: [https://doi.org/10.1016/0019-1035\(73\)90111-5](https://doi.org/10.1016/0019-1035(73)90111-5)

- Beatty, T. G. 2022, *Monthly Notices of the Royal Astronomical Society*, 513, 2652, doi: [10.1093/mnras/stac469](https://doi.org/10.1093/mnras/stac469)
- Benford, J. N., & Benford, D. J. 2016, *The Astrophysical Journal*, 825, 101, doi: [10.3847/0004-637X/825/2/101](https://doi.org/10.3847/0004-637X/825/2/101)
- Berdugina, S. V., & Kuhn, J. R. 2019, *The Astronomical Journal*, 158, 246, doi: [10.3847/1538-3881/ab2df3](https://doi.org/10.3847/1538-3881/ab2df3)
- Bracewell, R. N. 1960, *Nature*, 186, 670, doi: [10.1038/186670a0](https://doi.org/10.1038/186670a0)
- Bryson, S., Kunimoto, M., Kopparapu, R. K., et al. 2020, *The Astronomical Journal*, 161, 36, doi: [10.3847/1538-3881/abc418](https://doi.org/10.3847/1538-3881/abc418)
- Carroll-Nellenback, J., Frank, A., Wright, J., & Scharf, C. 2019, *The Astronomical Journal*, 158, 117, doi: [10.3847/1538-3881/ab31a3](https://doi.org/10.3847/1538-3881/ab31a3)
- Ćirković, M. M. 2004, *Astrobiology*, 4, 225, doi: [10.1089/153110704323175160](https://doi.org/10.1089/153110704323175160)
- Ćirković, M. M., & Vukotić, B. 2008, *Origins of Life and Evolution of Biospheres*, 38, 535, doi: [10.1007/s11084-008-9149-y](https://doi.org/10.1007/s11084-008-9149-y)
- Crawford, I. A., & Schulze-Makuch, D. 2024, *Nature Astronomy*, 8, 44, doi: [10.1038/s41550-023-02134-2](https://doi.org/10.1038/s41550-023-02134-2)
- Drake, F. D. 1961, *Physics Today*, 14, 40, doi: [10.1063/1.3057500](https://doi.org/10.1063/1.3057500)
- Dyson, F. J. 1960, *Science (New York, N.Y.)*, 131, 1667, doi: [10.1126/science.131.3414.1667](https://doi.org/10.1126/science.131.3414.1667)
- Enriquez, J. E., Siemion, A., Foster, G., et al. 2017, *The Astrophysical Journal*, 849, 104, doi: [10.3847/1538-4357/aa8d1b](https://doi.org/10.3847/1538-4357/aa8d1b)
- Gajjar, V., LeDuc, D., Chen, J., et al. 2022, *The Astrophysical Journal*, 932, 81, doi: [10.3847/1538-4357/ac6dd5](https://doi.org/10.3847/1538-4357/ac6dd5)
- Garrett, M. A., & Siemion, A. P. V. 2022, *Monthly Notices of the Royal Astronomical Society*, 519, 4581, doi: [10.1093/mnras/stac2607](https://doi.org/10.1093/mnras/stac2607)
- Grimaldi, C. 2017, *Scientific Reports*, 7, 46273, doi: [10.1038/srep46273](https://doi.org/10.1038/srep46273)
- Grimaldi, C. 2023, *The Astronomical Journal*, 165, 199, doi: [10.3847/1538-3881/acc327](https://doi.org/10.3847/1538-3881/acc327)
- Grimaldi, C., & Marcy, G. W. 2018, *Proceedings of the National Academy of Sciences*, 115, E9755, doi: [10.1073/pnas.1808578115](https://doi.org/10.1073/pnas.1808578115)
- Haqq-Misra, J., Kopparapu, R., Fauchez, T. J., et al. 2022a, *The Planetary Science Journal*, 3, 60, doi: [10.3847/PSJ/ac5404](https://doi.org/10.3847/PSJ/ac5404)
- Haqq-Misra, J., Schwieterman, E. W., Socas-Navarro, H., et al. 2022b, *Acta Astronautica*, 198, 194, doi: <https://doi.org/10.1016/j.actaastro.2022.05.040>
- Howard, A. W., Horowitz, P., Wilkinson, D. T., et al. 2004, *The Astrophysical Journal*, 613, 1270, doi: [10.1086/423300](https://doi.org/10.1086/423300)
- Jaiswal, B. 2023, *Astrobiology*, 23, 291, doi: [10.1089/ast.2022.0101](https://doi.org/10.1089/ast.2022.0101)
- Kopparapu, R., Arney, G., Haqq-Misra, J., Lustig-Yaeger, J., & Villanueva, G. 2021, *The Astrophysical Journal*, 908, 164, doi: [10.3847/1538-4357/abd7f7](https://doi.org/10.3847/1538-4357/abd7f7)
- Licquia, T. C., & Newman, J. A. 2016, *The Astrophysical Journal*, 831, 71, doi: [10.3847/0004-637X/831/1/71](https://doi.org/10.3847/0004-637X/831/1/71)
- Lin, H. W., Abad, G. G., & Loeb, A. 2014, *The Astrophysical Journal Letters*, 792, L7, doi: [10.1088/2041-8205/792/1/L7](https://doi.org/10.1088/2041-8205/792/1/L7)
- Lingam, M. 2016, *Astrobiology*, 16, 418, doi: [10.1089/ast.2015.1411](https://doi.org/10.1089/ast.2015.1411)
- Lingam, M., & Loeb, A. 2017a, *Monthly Notices of the Royal Astronomical Society: Letters*, 470, L82, doi: [10.1093/mnrasl/slx084](https://doi.org/10.1093/mnrasl/slx084)
- Lingam, M., & Loeb, A. 2017b, *The Astrophysical Journal Letters*, 837, L23, doi: [10.3847/2041-8213/aa633e](https://doi.org/10.3847/2041-8213/aa633e)
- Luan, X.-H., Tao, Z.-Z., Zhao, H.-C., et al. 2023, *The Astronomical Journal*, 165, 132, doi: [10.3847/1538-3881/acb706](https://doi.org/10.3847/1538-3881/acb706)
- Maire, J., Wright, S. A., Holder, J., et al. 2022, in *Ground-based and Airborne Instrumentation for Astronomy IX*, ed. C. J. Evans, J. J. Bryant, & K. Motohara, Vol. 12184, *International Society for Optics and Photonics (SPIE)*, 121848B, doi: [10.1117/12.2630772](https://doi.org/10.1117/12.2630772)
- Manunza, L., Vendrame, A., Pizzuto, L., et al. 2025, *Acta Astronautica*, 233, 155, doi: <https://doi.org/10.1016/j.actaastro.2025.04.007>
- Marcy, G. W., Tellis, N. K., & Wishnow, E. H. 2022, *Monthly Notices of the Royal Astronomical Society*, 515, 3898, doi: [10.1093/mnras/stac1933](https://doi.org/10.1093/mnras/stac1933)
- Margot, J.-L., Li, M. G., Pinchuk, P., et al. 2023, *The Astronomical Journal*, 166, 206, doi: [10.3847/1538-3881/acfda4](https://doi.org/10.3847/1538-3881/acfda4)
- Mason, L. A., Garrett, M. A., Wandia, K., & Siemion, A. P. V. 2024, *Monthly Notices of the Royal Astronomical Society*, 536, 2127, doi: [10.1093/mnras/stae2714](https://doi.org/10.1093/mnras/stae2714)
- McMillan, P. J. 2016, *Monthly Notices of the Royal Astronomical Society*, 465, 76, doi: [10.1093/mnras/stw2759](https://doi.org/10.1093/mnras/stw2759)
- Ng, C., Rizk, L., Mannion, C., & Keane, E. F. 2022, *The Astronomical Journal*, 164, 205, doi: [10.3847/1538-3881/ac92e7](https://doi.org/10.3847/1538-3881/ac92e7)
- Price, D. C., Enriquez, J. E., Brzycki, B., et al. 2020, *The Astronomical Journal*, 159, 86, doi: [10.3847/1538-3881/ab65f1](https://doi.org/10.3847/1538-3881/ab65f1)

- Seager, S., Welbanks, L., Ellerbroek, L., Bains, W., & Petkowski, J. J. 2025, Proceedings of the National Academy of Sciences, 122, e2416188122, doi: [10.1073/pnas.2416188122](https://doi.org/10.1073/pnas.2416188122)
- Siemion, A., Benford, J., Cheng-Jin, J., et al. 2015, in Advancing Astrophysics with the Square Kilometre Array, ed. T. L. Bourke, Vol. 215, 116, doi: [10.22323/1.215.0116](https://doi.org/10.22323/1.215.0116)
- Spiegel, D. S., & Turner, E. L. 2012, Proceedings of the National Academy of Sciences, 109, 395, doi: [10.1073/pnas.1111694108](https://doi.org/10.1073/pnas.1111694108)
- Suazo, M., Zackrisson, E., Wright, J. T., Korn, A. J., & Huston, M. 2022, Monthly Notices of the Royal Astronomical Society, 512, 2988, doi: [10.1093/mnras/stac280](https://doi.org/10.1093/mnras/stac280)
- Tarter, J. C., Agrawal, A., Ackermann, R., et al. 2010, in Instruments, Methods, and Missions for Astrobiology XIII, ed. R. B. Hoover, G. V. Levin, A. Y. Rozanov, & P. C. W. Davies, Vol. 7819, International Society for Optics and Photonics (SPIE), 781902, doi: [10.1117/12.863128](https://doi.org/10.1117/12.863128)
- Tremblay, C. D., & Tingay, S. J. 2024, The Astrophysical Journal, 972, 76, doi: [10.3847/1538-4357/ad6b11](https://doi.org/10.3847/1538-4357/ad6b11)
- Tremblay, C. D., Sofair, J., Steffes, L., et al. 2025, The Astronomical Journal, 169, 122, doi: [10.3847/1538-3881/ad9ea5](https://doi.org/10.3847/1538-3881/ad9ea5)
- Uno, Y., Hashimoto, T., Goto, T., et al. 2023, Monthly Notices of the Royal Astronomical Society, 522, 4649, doi: [10.1093/mnras/stad993](https://doi.org/10.1093/mnras/stad993)
- Włodarczyk-Sroka, B. S., Garrett, M. A., & Siemion, A. P. V. 2020, Monthly Notices of the Royal Astronomical Society, 498, 5720, doi: [10.1093/mnras/staa2672](https://doi.org/10.1093/mnras/staa2672)
- Wright, J. T., Kanodia, S., & Lubar, E. 2018, The Astronomical Journal, 156, 260, doi: [10.3847/1538-3881/aae099](https://doi.org/10.3847/1538-3881/aae099)